NeuroImage 58 (2011) 381–390

Contents lists available at ScienceDirect

NeuroImage

journal homepage: www.elsevier.com/locate/ynimg

Age-related changes in the surface morphology of the central sulcus

Shuyu Li [a,b], Mingrui Xia [b], Fang Pu [b], Deyu Li [b], Yubo Fan [b], Haijun Niu [a,b], Baoqing Pei [b], Yong He [c,*]

[a] State Key Laboratory of Software Development Environment, Beihang University, Beijing, China
[b] Key Laboratory for Biomechanics and Mechanobiology of Ministry of Education, School of Biological Science & Medical Engineering, Beihang University, Beijing, China
[c] State Key Laboratory of Cognitive Neuroscience and Learning, Beijing Normal University, Beijing, China

ARTICLE INFO

Article history:
Received 15 February 2011
Revised 23 May 2011
Accepted 16 June 2011
Available online 29 June 2011

Keywords:
Sulcal morphology
Central sulcus
Normal aging
Primary motor cortex
Primary sensory cortex

ABSTRACT

We utilized a sulcus-based computational approach to investigate the relationship between the three-dimensional (3D) morphology of the central sulcus (CS) and age. The anterior and posterior walls of the CS were manually outlined using high-resolution magnetic resonance images of 295 right-handed healthy participants (age range: 18 ~ 94 years). Surface reconstruction and parameterization methods were employed to create anatomical correspondence of surface locations across participants. Four surface metrics, including average sulcal length (SL), surface area, fractal dimension (FD) and sulcal span, were used to represent the 3D morphology of the CS. We found significant age-related decreases in the surface area for all walls of the CS, the SL for posterior walls of the CS and the FD for posterior wall of right CS. Age-related increases were found in the sulcal spans between the anterior and posterior walls. These surface metrics (except FD) exhibited leftward asymmetries. Specifically, age-related changes in surface morphology progressed more rapidly in the posterior than in the anterior walls. Finally, sex differences were found only in the FD of the right anterior wall of the CS. Taken together, our results show age-related changes in the surface morphology of the CS and therefore provide insights into the normal aging process.

Introduction

The central sulcus (CS), also known as the fissure of Rolando, is a prominent anatomical landmark of the brain. Conceptually, the CS is characterized by "a double S-shaped fissure that extends obliquely upward and backward on the lateral surface of each cerebral hemisphere of the brain and is located at the boundary between the frontal and parietal lobes" Anon (2007). The three-dimensional (3D) anatomy of the CS includes motor and sensory maps that are somatotopically organized according to Penfield's classical 'homunculus' (Penfield and Rasmussen, 1950). Studies of the CS are vital for exploring its morphological features and for determining the correspondence between its anatomy and function (Sastre-Janer et al., 1998). Previous neuroimaging studies have suggested that the 3D morphology of the CS can be influenced by many factors such as handedness (Amunts et al., 2000), sex (Amunts et al., 2000; Cykowski et al., 2008; Davatzikos and Bryan, 2002), genetics (Le Goualher et al., 2000), learning (Amunts et al., 1997; Li et al., 2010) and diseases (Fujiwara et al., 2007; Im et al., 2008).

Several recent studies have also examined the relationship between the 3D morphology of the CS and age; however, the results of these studies remain controversial and are under debate. For instance, Rettmann et al. (2006) measured the mean geodesic depths along the CS surface and found that there was no significant association between CS depth and age. However, Kochunov et al. (2005) reported that the depth of the CS became shallower and that the sulcal width increased with age. Moreover, Liu et al. (2010) showed that the width of the CS became larger with age. Notably, these previous studies mainly focused on the middle surface of the CS and neglected the morphology of the anterior (corresponding to the posterior wall of precentral gyrus) and posterior (corresponding to the anterior wall of postcentral gyrus) walls of the CS. The precentral and postcentral areas cytoarchitectonically differ, and these regions interact to contribute to motor and somatosensory functions, respectively. It is recognized that cortical thickness is normally greater in the precentral than in the postcentral gyrus, even within the same hemisphere (Butman and Floeter, 2007; MacDonald et al., 2000; Meyer et al., 1996). With respect to the aging, Salat et al. (2004) found that cortical thinning of the precentral gyrus was more rapid than that of the postcentral gyrus. Therefore, it is crucial to explore patterns of age-related changes in the anterior and posterior walls of the CS.

Here, we utilized a sulcus-based computational approach to investigate the relationship between the 3D morphology of the CS and age in a large cohort of healthy participants (n = 295, age range = 18–94 years). Given that sensorimotor abilities decline in older people (Calautti et al., 2001; Mattay et al., 2002; Sailer et al., 2000), we expected to observe age-related changes in CS morphology. To test our hypothesis, we first manually outlined the anterior and

* Corresponding author at: State Key Laboratory of Cognitive Neuroscience and Learning, Beijing Normal University, Beijing 100875, China. Fax: +86 10 58801023.
E-mail address: yong.he@bnu.edu.cn (Y. He).

1053-8119/$ – see front matter
doi:10.1016/j.neuroimage.2011.06.041

posterior walls of the CS from individual, high-resolution magnetic resonance (MR) images, followed by 3D surface reconstruction and parameterization. We then computed four surface metrics (average sulcal length (SL), surface area, fractal dimension (FD) and sulcal span) and examined age-related changes in the two walls of the CS.

Materials and methods

Participants

Three hundred and sixteen right-handed, healthy subjects were selected from the Open Access Series of Imaging Studies (OASIS) cross-sectional database (http://www.oasis-brains.org) (Marcus et al., 2007). Data from 21 subjects were excluded from further analysis because of failures of image preprocessing and sulcal surface reconstruction. The remaining 295 subjects consisted of 109 males and 186 females, ranging from 18 to 94 years of age. All subjects were evaluated using the Mini-Mental State Examination (MMSE) (Folstein et al., 1975) and Clinical Dementia Ratings (CDR) (Morris, 1993; Morris et al., 2001). MMSE scores were higher than 29, and CDR scores were all zero. For demographic data on all subjects, see Marcus et al. (2007). This dataset has been used in several previous studies (Bakkour et al., 2009; Dickerson et al., 2009; Fjell et al., 2009; He et al., 2008; Salat et al., 2009).

Image acquisition

For each subject, three to four individual T1-weighted magnetization prepared rapid gradient echo (MP-RAGE) images were acquired on a 1.5 T Vision scanner (Siemens, Erlangen, Germany) within a single session. Head movement was minimized by cushioning and a thermoplastic facemask. Images were motion corrected and averaged to create a single image with a high contrast-to-noise ratio. MP-RAGE parameters were empirically optimized for gray/white contrast: TR = 9.7 ms; TE = 4 ms; flip angle = 10°; slice number = 128; resolution = 256 × 256 (1 × 1 mm); thickness = 1.25 mm.

Extraction of CS

All native MR images were registered into stereotaxic space (Talairach, 1988) using a linear transformation (Collins et al., 1994). Images were simultaneously corrected for nonuniformity artifacts using N3 algorithms (Sled et al., 1998). The resulting images were used to extract the boundary of the CS with MRIcro (http://www.mricro.com) software. A neuroanatomy atlas (Duvernoy, 1999) was referred to for criteria used in delineating the CS, which were used in our recent study (Li et al., 2010). Briefly, the boundaries of the CS (including anterior and posterior boundaries) in each axial plane were drawn as a line beginning at the surface of the brain, outlining the posterior wall of the precentral gyrus (corresponding to the anterior wall of the CS) and the anterior wall of the postcentral gyrus (corresponding to the posterior wall of the CS). Fig. 1A shows the outlined anterior and posterior walls of the CS in a horizontal section from one representative subject. To estimate the reliability of measures based on manual outlining, two raters blind to the side of the brain being analyzed (left or right) traced both walls of the CS on twenty randomly selected brain volumes. Correlation coefficients between the raters for the SLs of the anterior and posterior walls of the CS were 0.91 and 0.90, respectively. Mean correlation coefficients for individual raters, based on measurements of the SLs of both walls, were 0.92 and 0.91, respectively.

Surface reconstruction of CS

The extracted CS outlines were represented as series of dispersed points in Talairach space (see Fig. 1B) and did not have spatial correspondence across subjects. It would be difficult to analyze the morphology of the CS based on these discrete points and to directly compare the morphological differences at each location of the CS between individuals. To address this issue, we employed a surface reconstruction and parameterization method to: 1) produce a surface representation based on the outlined CS boundary and 2) construct a uniform expression of each sulcal surface and build the anatomical correspondences among individuals (Thompson et al., 1996). The parameterization procedure was to divide each outlined cross-sectional contour into u partitions, each of which had the same arc length. Thus, the points with the same assigned indices on each cross-sectional contour constituted a curve along the lateral axis of Talairach space, which was further uniformly segmented into v partitions based on arc length. The details of the mesh construction algorithm have been described previously (Thompson et al., 1996, 1998). This method was also applied in our recent study (Li et al., 2010). Lastly, we constructed a uniform expression of $u \times v$ grids on different surfaces. Here, u ranged from 1 to 100, and v ranged from 1 to 150. Fig. 1C shows the 3D morphology of the anterior and posterior walls of the left CS in a representative subject.

Surface-based measurements

Average sulcal length and surface area

SL and surface area were used to describe the entire morphometry of CS surfaces. The SL was defined as the average length along the

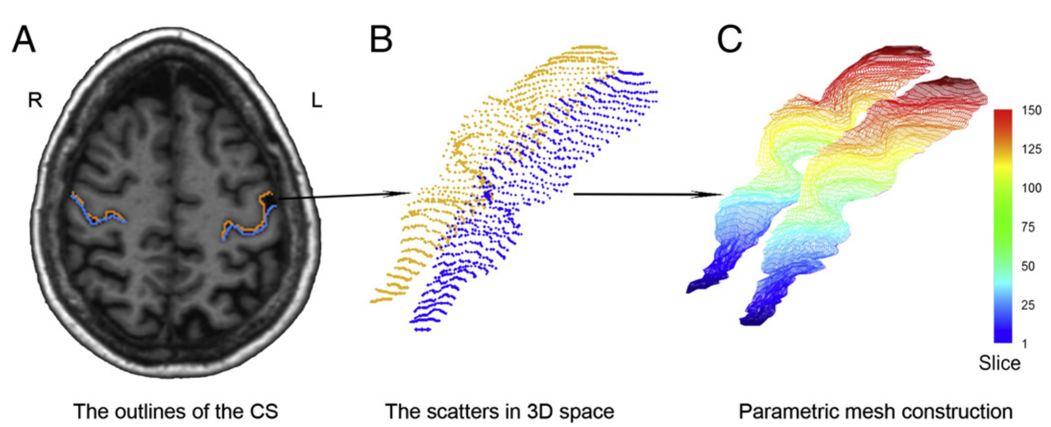

Fig. 1. A flowchart for surface construction of the CS. A. Outlines of the anterior (i.e., posterior walls of the precentral gyrus, yellow lines) and posterior (i.e., anterior walls of the postcentral gyrus, blue lines) walls of the CS in one representative subject. B. Scatter gram of the extracted anterior (yellow points) and posterior (blue points) walls of the CS. C. Parametric surface reconstruction of the anterior and posterior walls of the left CS. The blue–red hue scale indicates changes from the inferior to the superior CS.

exterior and interior sulcal boundaries of CS. Surface area was calculated by summing the areas of all grids in the parameterized surface, where the area of a grid was defined as the sum of the areas of two triangles within the grid.

Fractal dimension

We used FD to capture the complexity of the CS, which could estimate the degree of convolution of the CS surface. The FD was calculated using the box-counting method, which was similar to the study of Thompson et al. (1996). The CS was parameterized as an ordered hierarchy of meshes (S_{uv}) with variable resolution $u \times v$ ($u = 2$ to 100). Let $A(S_{uv})$ represent the surface area of the mesh S_{uv}, the FD was computed according to the formula: $2 - \{\partial \ln A(S_{uv}) / \partial \ln(1/u)\}$. The gradient was estimated by fitting a straight line by least squares regression of $\ln A(S_{uv})$ against $\ln(1/u)$, over the range $2 \leq u \leq 100$. A sulcus with extensive folding has a large FD, whereas a sulcus with smooth folding has a small FD.

Average span

The average span was defined as the average distance between the anterior and posterior walls of the CS, which could be related to regional atrophy of the postcentral and precentral areas (Kochunov et al., 2008). We first calculated the distance between each pair of corresponding points on the anterior and posterior walls of the CS and then averaged the 15,000 lengths to obtain the average span of the CS.

Asymmetry index

For each measurement, we computed the asymmetry index according to $(R - L)/[0.5 \times (R + L)]$, where R and L represent the separate measurements of the right and left hemispheres, respectively. A negative value indicates a leftward asymmetry, whereas a positive value indicates a rightward asymmetry.

Statistical analysis

To determine whether the surface measurements of the CS had significant associations with age, we performed a multiple linear regression analysis, in which each surface measurement was treated as a dependent variable, whereas age, sex and the interaction of age and sex were treated as independent variables. Several previous studies have shown the effects of sex on the 3D morphology of the CS (Amunts et al., 2000; Cykowski et al., 2008; Davatzikos and Bryan, 2002). We therefore took sex into account as a factor in our analyses. To determine whether the changes of the span between the anterior and posterior walls with normal aging were different along the surface, we analyzed the age-related variations for the span by multiple linear regression analysis in a vertex-by-vertex manner. In this analysis, a false discovery rate procedure was used to correct multiple comparisons (Genovese et al., 2002). Asymmetry scores were analyzed using a one-sample t-test to determine whether scores were significantly different from 0. Asymmetry scores for each measurement were also subjected to a MLR model to assess age-related changes, an analysis for which sex was also considered.

Results

Surface morphology of the CS

Age-related changes in CS surface morphology

Average sulcal length. Table 1 shows the measurements and statistical analyses results of the SL of the anterior and posterior walls of the CS. *Anterior walls:* there were trends toward age-related changes in the SL of anterior walls of the bilateral CS (left: $P = 0.089$; right: $P = 0.072$). *Posterior walls*: There were significant, bilateral decreases in the SL of the posterior wall of the CS (left: $P = 0.017$; right: $P = 0.0023$) with increasing age. The rates of decreases, for the left and right CS were 0.065 mm/year and 0.077 mm/year, respectively. We also found that the SL of the anterior walls of the CS was longer than that of the posterior walls (both $P < 0.001$). The rates of decreases with aging in the SL of the posterior walls were faster than those in the anterior walls for both hemispheres. Scatter plots are shown in Fig. 2.

Surface area. Table 2 shows the surface areas of the anterior and posterior walls of the CS. *Anterior walls:* the bilateral surface areas of the anterior walls of the CS showed significant reduction with increasing age (left: $P = 0.026$; right: $P < 0.001$). For the left and right hemispheres, the decreases were 1.78 mm^2/year and 2.26 mm^2/year, respectively. *Posterior walls*: age-related reductions in surface area were also significant in the posterior walls of the CS in both hemispheres (both $P < 0.001$). The rates of decrease were 3.63 mm^2/year and 3.15 mm^2/year for the left and right CS, respectively. We found that the surface area of the anterior walls of the CS was larger than those of the posterior walls (both $P < 0.001$) for both hemispheres. However, age-related reductions were more rapid bilaterally in the posterior wall than in the anterior wall of the CS. Scatter plots are shown in Fig. 3.

Fractal dimension. Table 3 presents the regression results for the FD of the anterior and posterior walls of the CS. *Anterior walls:* there were trends toward age-related changes in the FD of the anterior walls of the bilateral CS (left: $P = 0.070$; right: $P = 0.062$). *Posterior walls*: there were significant reductions in the FD of posterior wall of the right CS ($P = 0.0052$) with increasing age. There were no age-related changes in the FD of the posterior wall of the left CS ($P = 0.12$). The FD of the

Table 1
Average sulcal lengths of the anterior and posterior walls of the CS.

Position	Age		Sex			Interaction
	Beta (mm/year)	*P*	Male mean (mm) (STD)	Female mean (mm) (STD)	*P*	*P*
AL	−0.047	0.089	146.66 (10.68)	146.91 (10.18)	0.64	0.80
AR	−0.047	0.072	140.34 (525.82)	141.23 (466.24)	1.00	0.58
PL	−0.065	0.017*	142.25 (10.81)	141.56 (9.94)	0.40	0.31
PR	−0.077	0.0023**	138.52 (8.89)	137.99 (9.87)	0.51	0.44

AL represents the anterior wall of the left CS; AR represents the anterior wall of the right CS; PL represents the posterior wall of the left CS; PR represents the posterior wall of the right CS.
* $P < 0.05$.
** $P < 0.01$.

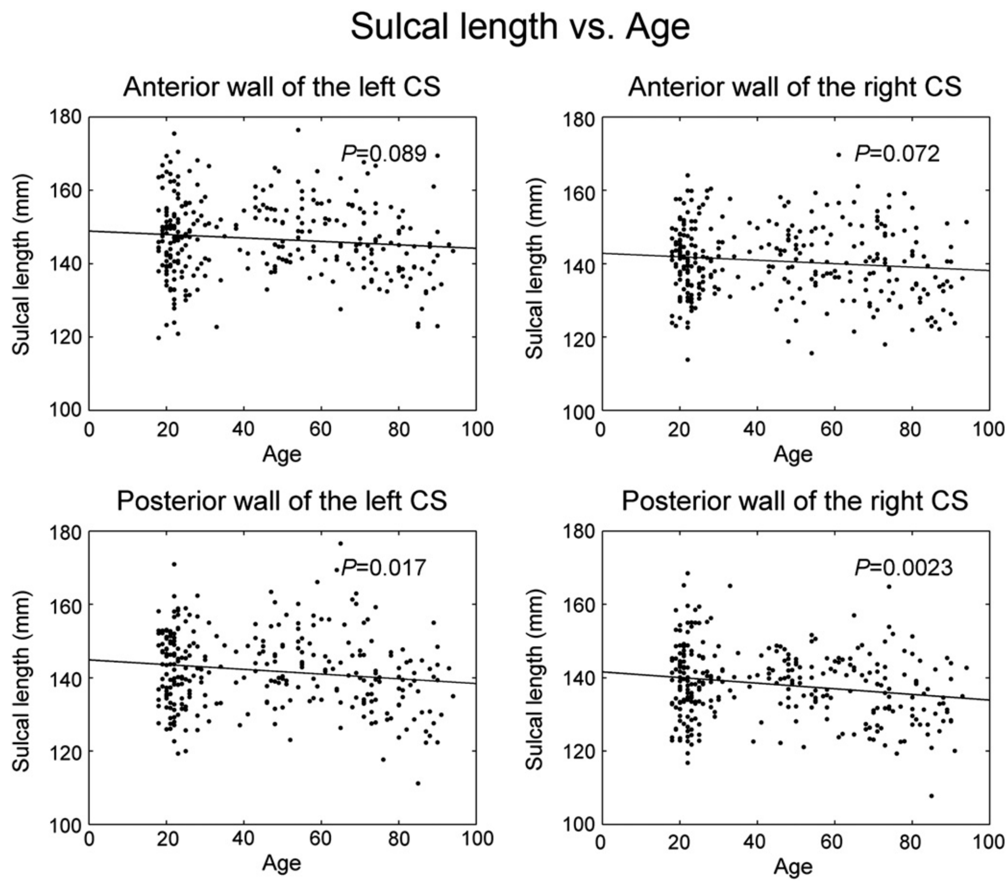

Fig. 2. Scatter plots for average sulcal length of the CS. Black points represent subjects.

anterior walls of the bilateral CS did not show significant differences as compared to those of the posterior walls (both $P>0.05$). Also, the decrease rates with aging did not show significant differences between both walls of bilateral CS. Scatter plots are shown in Fig. 4.

Average span. Age-related changes in the average span between the anterior and posterior walls are shown in Table 4. The average span showed significant widening, with an increase of 0.025 mm/year for the left hemisphere and 0.023 mm/year for the right hemisphere (both $P<0.001$). Scatter plots are shown in Fig. 5. We also performed a vertex-based analysis to detect age-related changes in the span between the anterior and posterior walls (Fig. 6A). The results of this analysis indicated that there was significant, bilateral widening (corrected $P<0.05$) in the upper and lower sections of the CS. In the present study, we also examined the change in the spatial coordinates for each vertex on the anterior and posterior walls of the CS. Vertex-based displacements of the anterior and posterior walls over time are shown in the Supplementary Video. We found significant forward movements bilaterally (corrected $P<0.05$) in the upper and lower sections of the anterior walls of the CS with increasing age (Fig. 6B), whereas significant, bilateral backward movements (corrected $P<0.05$) appeared bilaterally in the middle section of the posterior walls of the CS (Fig. 6C).

Sex-related differences in morphology of the CS

Sex differences are shown in Tables 1–4. The only sex difference we observed was that females displayed a larger right anterior FD than males ($P=0.032$). We also found the interaction between age

Table 2
Surface areas of the anterior and posterior walls of the CS.

Position	Age		Sex			Interaction
	Beta (mm^2/year)	P	Male mean (mm^2) (STD)	Female mean (mm^2) (STD)	P	P
AL	−1.78	0.026*	2579.11 (280.11)	2612.03 (314.76)	0.38	0.77
AR	−2.26	9.58×10^{-4}***	2506.00 (256.27)	2504.04 (261.14)	0.21	0.10
PL	−3.63	1.37×10^{-9}***	2455.56 (225.99)	2448.82 (239.08)	0.62	0.90
PR	−3.15	6.25×10^{-8}***	2373.40 (217.22)	2353.50 (228.70)	0.42	0.32

AL represents the anterior wall of the left CS; AR represents the anterior wall of the right CS; PL represents the posterior wall of the left CS; PR represents the posterior wall of the right CS.
* $P<0.05$.
*** $P<0.001$.

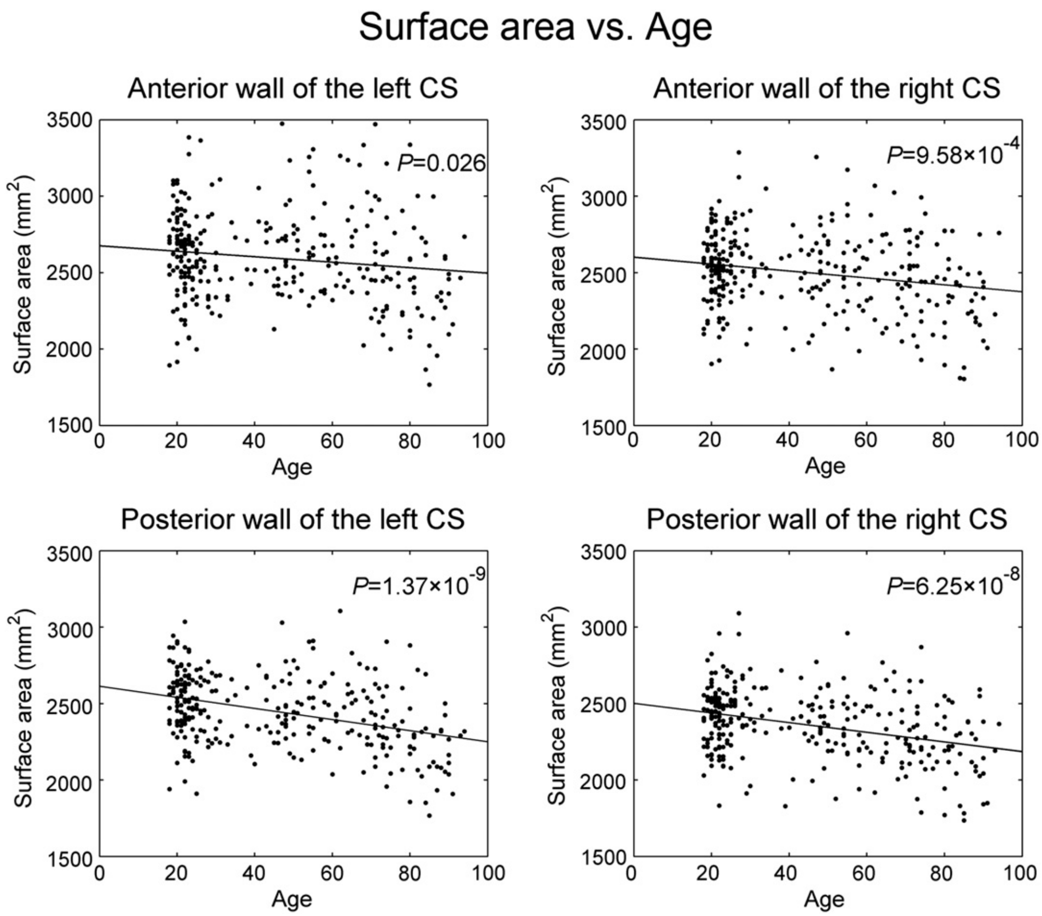

Fig. 3. Scatter plots for surface area of the CS. Black points represent subjects.

and sex factors in the FD of anterior wall of the right CS ($P=0.0072$), in which the decreases of FD of males were faster than those of females with normal aging. No interactions between age and sex factors were observed for other surface measurements of the anterior and posterior walls of the CS for either hemisphere ($P>0.09$).

Asymmetry of morphological measurements of the CS

A one-sample *t* test revealed significant leftward asymmetries in the SL and surface area of the anterior and posterior walls of the CS. Table 5 presents age- and sex-related changes in the asymmetry indices. We found no significant decreases with aging in the asymmetries of any measurements for both walls of bilateral CS (all $P>0.4$). There were significant sex differences in the asymmetry indices of the surface area of the anterior wall of the CS ($P=0.038$), for which females had more leftward asymmetry than males. The average span showed more leftward asymmetry in females than in males.

Validation of results

To validate the effects of CS orientations on the age-related changes of CS morphological measures, we conducted respectively 5000 random experiments for both walls of bilateral CS of each subject. In each experiment, we assigned a random rotation angle

Table 3
FDs of the anterior and posterior walls of the CS.

Position	Age		Sex			Interaction
	Beta (1/year)	P	Male mean (STD)	Female mean (STD)	P	P
AL	-3.30×10^{-5}	0.070	2.020 (0.0063)	2.021 (0.0071)	0.94	0.68
AR	-2.81×10^{-5}	0.062	2.033 (0.0055)	2.033 (0.0058)	0.032*	0.0072**
PL	-2.19×10^{-5}	0.120	2.023 (0.0054)	2.024 (0.0041)	0.52	0.16
PR	-3.02×10^{-5}	0.0052**	2.032 (0.0041)	2.031 (0.0041)	0.48	0.80

AL represents the anterior wall of the left CS; AR represents the anterior wall of the right CS; PL represents the posterior wall of the left CS; PR represents the posterior wall of the right CS.
* $P<0.05$.
** $P<0.01$.

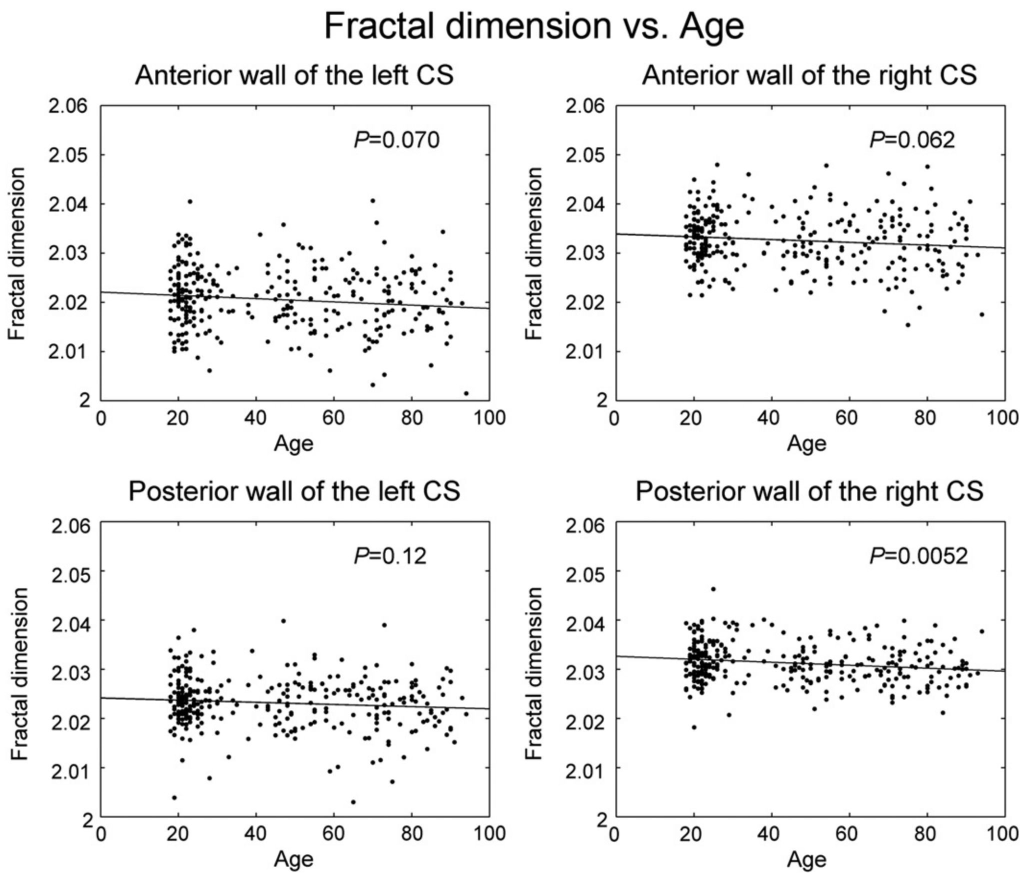

Fig. 4. Scatter plots for fractal dimension of the CS. Black points represent subjects.

(range: $-10°$ to $10°$, followed by the distribution of uniform possibility density function) around the X axis (i.e., left–right direction) for each CS. Then, we computed the surface area and SL, and analyzed the associations among these measures and age. We found 2720 times (i.e., 54.40%) significant age-related reductions for SL of posterior wall of the left CS, and 4335 times (i.e., 86.70%) for posterior wall of the right CS. The significant age-related reductions in 4084 times (i.e., 81.68%) experiments were found in the surface area of anterior wall of the left CS, and in all 5000 times (i.e., 100%) experiments in the surface area of anterior wall of the right CS and posterior walls of bilateral CS. Notably, the age-related reductions in the SL for posterior wall of the left CS needed to be cautious. The reliability rates for age-related changes for the surface area of anterior wall of the right CS and posterior wall of bilateral CS were 100%. More detailed experiments are shown in Supplementary materials.

Discussion

In this study, we employed a sulcal mapping method to investigate the morphological changes of the anterior and posterior walls of the CS during normal aging. The average SL, surface area, FD and average span were calculated to represent the morphology of the CS on the basis of reconstructed surface meshes. SL showed significant decreases in bilateral posterior walls of the CS, whereas the surface areas of both hemispheres showed significant reductions in each wall of the CS during normal aging. FD showed age-related reductions only in the posterior wall of right CS. The average span between the anterior and posterior walls of the CS showed significant, bilateral increases with aging. Furthermore, the rates of decreases of these measurements (except FD) with age were higher in the posterior walls than those in the anterior walls. Taken together, our results provide evidence for the morphological variations of the anterior and posterior walls of the CS during normal aging.

Age-related changes in CS morphology

We found that the majority of the measurements (SL, surface area and FD) of both walls of the CS showed significant, bilateral decreases with age. Several previous studies have examined age-related morphological changes of the CS, but the findings remain controversial. For

Table 4
Average, bilateral span of the CS.

Position	Age		Sex			Interaction
	Beta (mm/year)	P	Male mean (mm) (STD)	Female mean (mm) (STD)	P	P
Left CS	0.025	1.00×10^{-16}***	3.01 (1.08)	3.40 (1.21)	0.60	0.81
Right CS	0.023	1.44×10^{-15}***	3.17 (1.13)	3.34 (1.23)	0.27	0.25

*** $P<0.001$.

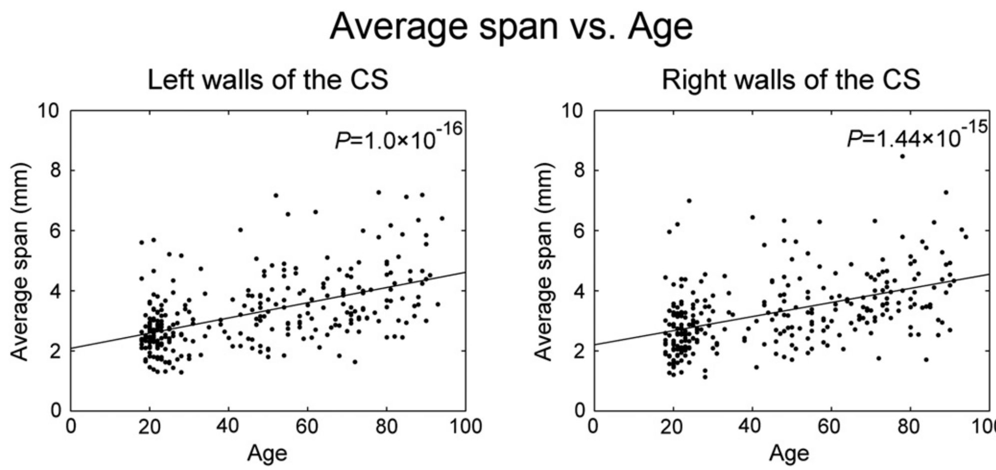

Fig. 5. Scatter plots for average span of the CS. Black points represent subjects.

example, Rettmann et al. (2006) did not find a correlation between the mean depth of the CS and age in 35 subjects, with subject age ranging from 59 to 84 years. Similarly, Cykowski et al. (2008) did not find a significant relationship between age and mean CS depth. However, Kochunov et al. (2005) measured the average sulcal depth of the CS in 90 subjects between 20 and 82 years of age and found that the average sulcal depth of the CS significantly decreased with age. Liu et al. (2010) investigated CS morphology in 319, non-demented individuals between 70 and 90 years of age and found that the average span of the CS became larger with age. These findings are in line with our results. Sulcal morphology is thought to be intimately tied to regional reduction in gray matter (GM) and white matter (WM) gyral volumes. Many studies have found age-related GM reductions in the pre- and postcentral gyrus (Good et al., 2001; Taki et al., 2004) and WM abnormalities in the frontal and parietal cortices (Abe et al., 2008; Salat et al., 2005; Wu et al., 2010). We speculate that age-related changes in CS morphology may be related to the declines of frontal and parietal cortices during normal aging.

Sex-related differences in CS morphology

In this study, the only significant sex difference we observed was that females presented a larger FD in the anterior wall of the right CS than males. But the decreases of FD of males were faster than those of females with normal aging. Several previous studies have examined sex-related differences in CS morphology, but the findings are still a point of contention. For instance, Cykowski et al. (2008) found no significant sex differences in location and depth of the CS using sulcal surface measurements. Kochunov et al. (2005) found significant sex differences in sulcal widths of the superior temporal, collateral and cingulate sulci, but not in the CS. However, Liu et al. (2010) found that men had a significantly wider sulcal span in the CS than women. Inconsistencies between studies may be explained by the discrepancies in both the applied methodology and the age ranges of the participants.

Asymmetries of CS morphological measurements

We found significant leftward asymmetries in the SL and surface area of the anterior and posterior walls of the CS in the right-handed subjects. These findings are compatible with previous studies (Amunts et al., 1997; Cykowski et al., 2008; Li et al., 2010; Mangin et al., 2004). We also noted significant sex differences in the asymmetries of surface area of the anterior walls of the CS and the average span, in which females showed more leftward asymmetries than males. Sex differences in CS asymmetry are in dispute. For example, Amunts et al. (2000) found that depths of the CS in females were more symmetric than those in males. However, White et al. (1997b) found that the asymmetry of the human primary sensorimotor system was not significantly different between the genders. Sulcal asymmetry is considered to be related to corpus callosum size (Luders et al., 2003). If a processing task predominantly occurs in a single hemisphere, there may be less need for interhemispheric information exchange. This hemispheric dominance could be related to a decreased callosal size, and therefore, a negative correlation may exist between functional lateralization and callosal size. However,

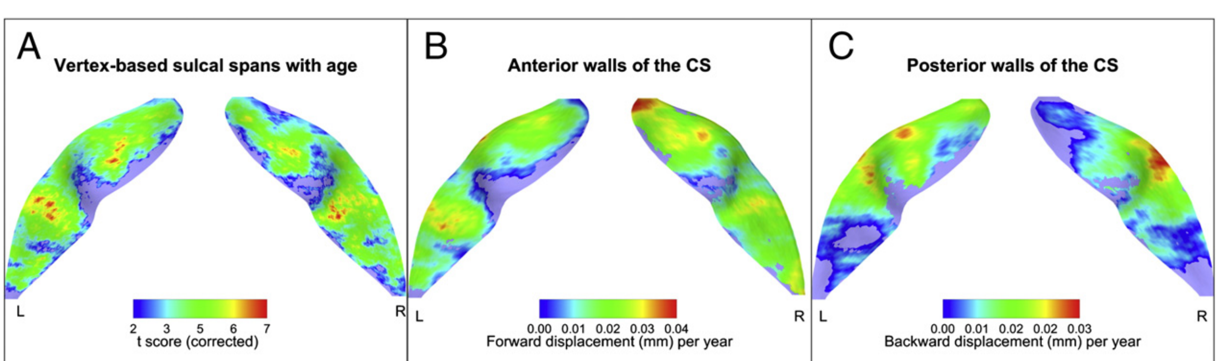

Fig. 6. Changes of vertex-based sulcal spans with age. A. Vertex-based sulcal span with age; regions with significant positive correlations ($t>2.0$, $P<0.05$) were mapped on the average surface of the CS. No significant negative correlations were found. B. Local forward displacement of the anterior walls of the CS per year. C. Local backward displacement of the posterior walls of the CS per year. L, left hemisphere; R, right hemisphere.

Table 5
Asymmetry indices of surface measurements of the anterior and posterior walls of the CS.

Measurements	Position	Age		Sex			Interaction
		Beta	*P*	Male mean (STD)	Female mean (STD)	*P*	*P*
SL	Anterior	-2.90×10^{-5}	0.89	−0.044 (0.083)	−0.039 (0.077)	0.69	0.48
	Posterior	-7.95×10^{-5}	0.69	−0.026 (0.079)	−0.026 (0.072)	0.14	0.096
Area	Anterior	-1.99×10^{-4}	0.48	−0.028 (0.112)	−0.040 (0.104)	0.038*	0.06
	Posterior	-1.57×10^{-4}	0.49	−0.034 (0.086)	−0.040 (0.804)	0.173	0.25
FD	Anterior	-2.48×10^{-6}	0.81	0.0061 (0.0038)	0.0059 (0.0040)	0.11	0.12
	Posterior	-4.05×10^{-6}	0.62	0.0040 (0.0032)	0.0035 (0.0029)	0.93	0.17
Span		-5.03×10^{-4}	0.52	0.051 (0.329)	−0.025 (0.273)	0.024*	0.15

* $P<0.05$.

data concerning sexual dimorphism of the corpus callosum are contradictory and are currently debated (Luders et al., 2003). Further studies on sex differences in the asymmetry of the CS are needed.

Anterior versus posterior walls

We found that morphological measurements (i.e., SL and surface area) of the anterior walls of the CS were much larger than those of the posterior walls. The precentral and postcentral areas cytoarchitectonically differ and interact to contribute to motor and somatosensory functions. It is recognized that within an individual, precentral thickness is normally greater than postcentral thickness in the same hemisphere (Butman and Floeter, 2007; MacDonald et al., 2000; Meyer et al., 1996). White et al. (1997a) reported larger cortical volume in the precentral gyrus compared to the postcentral gyrus. Our results were consistent with the above studies. However, we found that the decreases of these measurements with age in the posterior walls of the CS were more rapid than those in the anterior walls. There are few studies that compare age-related rates of decline of the precentral and postcentral gyrus, and the existing findings are not consistent. For example, Salat et al. (2004) investigated cortical thickness changes in aging and found significant thinning in precentral and postcentral gyri, and also found that the rates of cortical thickness thinning in the precentral gyrus were faster than that in the postcentral gyrus. However, Raz et al. (1997) examined age-related changes in pre- and postcentral gyrus volumes in 148 healthy subjects with ages ranging from 18 to 77 years and found that GM volumes of the precentral cortex had no correlation with age, but those of postcentral cortex showed significant negative correlations with age. These findings are partially line with ours, and may be explained by the study of Adams (1987). This group found that the motor cortex was capable of synaptic plasticity in response to aging-induced synaptic loss, but they did not observe this phenomenon in the somatosensory cortex. Age-related decline patterns of the motor and somatosensory cortices should be investigated in the future.

Comparisons of morphological measurements

In this study, we employed four measures (i.e., average SL, surface area, FD and average sulcal span) to characterize the CS morphology from different views. The average SL was measured along the exterior and interior sulcal boundaries. The surface area was measured by computing the area of the whole sulcal surface. The SL did not show a close relationship with surface area for either CS surface. Moreover, we used FD to capture the complexity of the CS, which could estimate the degree of convolution of the CS surfaces. FD is an extremely compact measure of shape complexity, condensing all details into a single numeric value and has been used to describe the geometrical properties of cortex and sulci (Im et al., 2006; Jiang et al., 2008). The average span was defined as the average distance between the anterior and posterior walls of the CS, which was similar to the sulcal width proposed by Kochunov et al. (2005). It would be larger with the atrophy of the postcentral and precentral areas. Among these measurements, we found that the surface area metric was more sensitive to the detection of age-related changes than other metrics. In future, other rigorous geometric measures, such as average curvedness (Awate et al., 2009), could be applied to investigate the age-related changes of the convolution of the CS. The combination of these surface measurements is vital and necessary for aging studies because different surface metrics reflect distinct aspects of brain morphology.

Further considerations

Several issues need to be addressed further. First, a cross-sectional database was employed in this study, which limited the interpretation of correlation analyses. Longitudinal studies could track the dynamic process of brain degeneration in normal aging and provide direct evidence of brain changes with age. Thus, it will be important to validate the age-related changes of the CS in a longitudinal database. Second, we drew the boundaries of anterior and posterior walls of the CS by manual, and the measures of CS morphology depended on the orientation of the scan. In future, more accurate 3D segmentation method for anterior and posterior walls of the CS should be used to extract the surfaces of the CS in order to avoid the problem of orientation dependence. Third, sulcal parameterization is a critical step in investigating sulcal morphology. In this study, we employed the method of Thompson et al. (1996), which has proven to be capable of characterizing variations in sulcal geometry (Levitt et al., 2003; Li et al., 2010; Thompson et al., 1998). However, other sulcal reconstruction and parameterization methods have been proposed (Clouchoux et al., 2005; Coulon et al., 2006). In future studies, it would be meaningful to compare the findings of these parameterization methods on differences in sulcal geometry. Fourth, we found different age-related changes in the anterior and posterior walls of the CS. This individual sulcal mapping method could be used to analyze the morphology of those sulci in which the anterior and posterior walls have different functions, such as the Sylvian fissure. Finally, it would be interesting to investigate CS morphology in patients with abnormal motor function, such as stroke, attention deficit hyperactivity disorder and Parkinson's disease.

Conclusion

In this study, we employed a sulcal geometry-based statistical analysis approach to investigate age-related changes in CS morphology in a large cohort of healthy participants. The major advantage of this sulcal mapping method was that it was capable of capturing subtle structural adaptations in the morphology of the CS in normal aging. Our results strongly suggest that the anterior and posterior walls of the CS undergo different age-related change patterns, thus providing insight into the understanding of normal brain aging.

Supplementary materials related to this article can be found online at doi:10.1016/j.neuroimage.2011.06.041.

Acknowledgments

This work was supported by the National Science Foundation of China (Nos. 30700182, 81071212, 81030028, and 30870667), State Key Laboratory of Software Development Environment (No. SKLSDE-2011ZX-10), the Beijing Natural Science Foundation (No. 7102090) and the Scientific Research Foundation for the Returned Overseas Chinese Scholars (State Education Ministry, YH).

References

Abe, O., Yamasue, H., Aoki, S., Suga, M., Yamada, H., Kasai, K., Masutani, Y., Kato, N., Ohtomo, K., 2008. Aging in the CNS: comparison of gray/white matter volume and diffusion tensor data. Neurobiol. Aging 29, 102–116.

Adams, I., 1987. Comparison of synaptic changes in the precentral and postcentral cerebral cortex of aging humans: a quantitative ultrastructural study. Neurobiol. Aging 8, 203–212.

Amunts, K., Schlaug, G., Jancke, L., Steinmetz, H., Schleicher, A., Dabringhaus, A., Zilles, K., 1997. Motor cortex and hand motor skills: structural compliance in the human brain. Hum. Brain Mapp. 5, 206–215.

Amunts, K., Jancke, L., Mohlberg, H., Steinmetz, H., Zilles, K., 2000. Interhemispheric asymmetry of the human motor cortex related to handedness and gender. Neuropsychologia 38, 304–312.

Anon, 2007. The American Heritage Medical Dictionary. Houghton Mifflin Co., Boston.

Awate, S.P., Yushkevich, P., Licht, D., Gee, J.C., 2009. Gender differences in cerebral cortical folding: multivariate complexity-shape analysis with insights into handling brain-volume differences. Med. Image Comput. Comput. Assist. Interv. 12, 200–207.

Bakkour, A., Morris, J.C., Dickerson, B.C., 2009. The cortical signature of prodromal AD: regional thinning predicts mild AD dementia. Neurology 72, 1048–1055.

Butman, J.A., Floeter, M.K., 2007. Decreased thickness of primary motor cortex in primary lateral sclerosis. AJNR Am. J. Neuroradiol. 28, 87–91.

Calautti, C., Serrati, C., Baron, J.C., 2001. Effects of age on brain activation during auditory-cued thumb-to-index opposition: a positron emission tomography study. Stroke 32, 139–146.

Clouchoux, C., Coulon, O., Riviere, D., Cachia, A., Mangin, J.F., Regis, J., 2005. Anatomically constrained surface parameterization for cortical localization. Med. Image Comput. Comput. Assist. Interv. 8, 344–351.

Collins, D.L., Neelin, P., Peters, T.M., Evans, A.C., 1994. Automatic 3D intersubject registration of MR volumetric data in standardized Talairach space. J. Comput. Assist. Tomogr. 18, 192–205.

Coulon, O., Clouchoux, C., Operto, G., Dauchot, K., Sirigu, A., Anton, J.-I., 2006. Cortical localization via surface parameterization: a sulcus-based approach. NeuroImage 31, S46.

Cykowski, M.D., Coulon, O., Kochunov, P.V., Amunts, K., Lancaster, J.L., Laird, A.R., Glahn, D.C., Fox, P.T., 2008. The central sulcus: an observer-independent characterization of sulcal landmarks and depth asymmetry. Cereb. Cortex 18, 1999–2009.

Davatzikos, C., Bryan, R.N., 2002. Morphometric analysis of cortical sulci using parametric ribbons: a study of the central sulcus. J. Comput. Assist. Tomogr. 26, 298–307.

Dickerson, B.C., Bakkour, A., Salat, D.H., Feczko, E., Pacheco, J., Greve, D.N., Grodstein, F., Wright, C.I., Blacker, D., Rosas, H.D., Sperling, R.A., Atri, A., Growdon, J.H., Hyman, B.T., Morris, J.C., Fischl, B., Buckner, R.L., 2009. The cortical signature of Alzheimer's disease: regionally specific cortical thinning relates to symptom severity in very mild to mild AD dementia and is detectable in asymptomatic amyloid-positive individuals. Cereb. Cortex 19, 497–510.

Duvernoy, H. (Ed.), 1999. The Human Brain: Surface, Blood Supply, and Three-Dimensional Sectional Anatomy, 2nd ed. Springer, Wien:.

Fjell, A.M., Westlye, L.T., Amlien, I., Espeseth, T., Reinvang, I., Raz, N., Agartz, I., Salat, D.H., Greve, D.N., Fischl, B., Dale, A.M., Walhovd, K.B., 2009. High consistency of regional cortical thinning in aging across multiple samples. Cereb. Cortex 19, 2001–2012.

Folstein, M.F., Folstein, S.E., McHugh, P.R., 1975. Mini-mental state. A practical method for grading the cognitive state of patients for the clinician. J. Psychiatr. Res. 12, 189–198.

Fujiwara, H., Hirao, K., Namiki, C., Yamada, M., Shimizu, M., Fukuyama, H., Hayashi, T., Murai, T., 2007. Anterior cingulate pathology and social cognition in schizophrenia: a study of gray matter, white matter and sulcal morphometry. NeuroImage 36, 1236–1245.

Genovese, C.R., Lazar, N.A., Nichols, T., 2002. Thresholding of statistical maps in functional neuroimaging using the false discovery rate. NeuroImage 15, 870–878.

Good, C.D., Johnsrude, I.S., Ashburner, J., Henson, R.N., Friston, K.J., Frackowiak, R.S., 2001. A voxel-based morphometric study of ageing in 465 normal adult human brains. NeuroImage 14, 21–36.

He, Y., Chen, Z., Evans, A., 2008. Structural insights into aberrant topological patterns of large-scale cortical networks in Alzheimer's disease. J. Neurosci. 28, 4756–4766.

Im, K., Lee, J.M., Yoon, U., Shin, Y.W., Hong, S.B., Kim, I.Y., Kwon, J.S., Kim, S.I., 2006. Fractal dimension in human cortical surface: multiple regression analysis with cortical thickness, sulcal depth, and folding area. Hum. Brain Mapp. 27, 994–1003.

Im, K., Lee, J.M., Seo, S.W., Hyung Kim, S., Kim, S.I., Na, D.L., 2008. Sulcal morphology changes and their relationship with cortical thickness and gyral white matter volume in mild cognitive impairment and Alzheimer's disease. NeuroImage 43, 103–113.

Jiang, J., Zhu, W., Shi, F., Zhang, Y., Lin, L., Jiang, T., 2008. A robust and accurate algorithm for estimating the complexity of the cortical surface. J. Neurosci. Methods 172, 122–130.

Kochunov, P., Mangin, J.F., Coyle, T., Lancaster, J., Thompson, P., Riviere, D., Cointepas, Y., Regis, J., Schlosser, A., Royall, D.R., Zilles, K., Mazziotta, J., Toga, A., Fox, P.T., 2005. Age-related morphology trends of cortical sulci. Hum. Brain Mapp. 26, 210–220.

Kochunov, P., Thompson, P.M., Coyle, T.R., Lancaster, J.L., Kochunov, V., Royall, D., Mangin, J.F., Riviere, D., Fox, P.T., 2008. Relationship among neuroimaging indices of cerebral health during normal aging. Hum. Brain Mapp. 29, 36–45.

Le Goualher, G., Argenti, A.M., Duyme, M., Baare, W.F., Hulshoff Pol, H.E., Boomsma, D.I., Zouaoui, A., Barillot, C., Evans, A.C., 2000. Statistical sulcal shape comparisons: application to the detection of genetic encoding of the central sulcus shape. NeuroImage 11, 564–574.

Levitt, J.G., Blanton, R.E., Smalley, S., Thompson, P.M., Guthrie, D., McCracken, J.T., Sadoun, T., Heinichen, L., Toga, A.W., 2003. Cortical sulcal maps in autism. Cereb. Cortex 13, 728–735.

Li, S., Han, Y., Wang, D., Yang, H., Fan, Y., Lv, Y., Tang, H., Gong, Q., Zang, Y., He, Y., 2010. Mapping surface variability of the central sulcus in musicians. Cereb. Cortex 20, 25–33.

Liu, T., Wen, W., Zhu, W., Trollor, J., Reppermund, S., Crawford, J., Jin, J.S., Luo, S., Brodaty, H., Sachdev, P., 2010. The effects of age and sex on cortical sulci in the elderly. NeuroImage 51, 19–27.

Luders, E., Rex, D.E., Narr, K.L., Woods, R.P., Jancke, L., Thompson, P.M., Mazziotta, J.C., Toga, A.W., 2003. Relationships between sulcal asymmetries and corpus callosum size: gender and handedness effects. Cereb. Cortex 13, 1084–1093.

MacDonald, D., Kabani, N., Avis, D., Evans, A.C., 2000. Automated 3-D extraction of inner and outer surfaces of cerebral cortex from MRI. NeuroImage 12, 340–356.

Mangin, J.F., Riviere, D., Cachia, A., Duchesnay, E., Cointepas, Y., Papadopoulos-Orfanos, D., Scifo, P., Ochiai, T., Brunelle, F., Regis, J., 2004. A framework to study the cortical folding patterns. NeuroImage 23 (Suppl 1), S129–S138.

Marcus, D.S., Wang, T.H., Parker, J., Csernansky, J.G., Morris, J.C., Buckner, R.L., 2007. Open Access Series of Imaging Studies (OASIS): cross-sectional MRI data in young, middle aged, nondemented, and demented older adults. J. Cogn. Neurosci. 19, 1498–1507.

Mattay, V.S., Fera, F., Tessitore, A., Hariri, A.R., Das, S., Callicott, J.H., Weinberger, D.R., 2002. Neurophysiological correlates of age-related changes in human motor function. Neurology 58, 630–635.

Meyer, J.R., Roychowdhury, S., Russell, E.J., Callahan, C., Gitelman, D., Mesulam, M.M., 1996. Location of the central sulcus via cortical thickness of the precentral and postcentral gyri on MR. AJNR Am. J. Neuroradiol. 17, 1699–1706.

Morris, J.C., 1993. The Clinical Dementia Rating (CDR): current version and scoring rules. Neurology 43, 2412–2414.

Morris, J.C., Storandt, M., Miller, J.P., McKeel, D.W., Price, J.L., Rubin, E.H., Berg, L., 2001. Mild cognitive impairment represents early-stage Alzheimer disease. Arch. Neurol. 58, 397–405.

Penfield, W., Rasmussen, T., 1950. The Cerebral Cortex of the Man. Macmillan, New York.

Raz, N., Gunning, F.M., Head, D., Dupuis, J.H., McQuain, J., Briggs, S.D., Loken, W.J., Thornton, A.E., Acker, J.D., 1997. Selective aging of the human cerebral cortex observed in vivo: differential vulnerability of the prefrontal gray matter. Cereb. Cortex 7, 268–282.

Rettmann, M.E., Kraut, M.A., Prince, J.L., Resnick, S.M., 2006. Cross-sectional and longitudinal analyses of anatomical sulcal changes associated with aging. Cereb. Cortex 16, 1584–1594.

Sailer, A., Dichgans, J., Gerloff, C., 2000. The influence of normal aging on the cortical processing of a simple motor task. Neurology 55, 979–985.

Salat, D.H., Buckner, R.L., Snyder, A.Z., Greve, D.N., Desikan, R.S., Busa, E., Morris, J.C., Dale, A.M., Fischl, B., 2004. Thinning of the cerebral cortex in aging. Cereb. Cortex 14, 721–730.

Salat, D.H., Tuch, D.S., Greve, D.N., van der Kouwe, A.J., Hevelone, N.D., Zaleta, A.K., Rosen, B.R., Fischl, B., Corkin, S., Rosas, H.D., Dale, A.M., 2005. Age-related alterations in white matter microstructure measured by diffusion tensor imaging. Neurobiol. Aging 26, 1215–1227.

Salat, D.H., Greve, D.N., Pacheco, J.L., Quinn, B.T., Helmer, K.G., Buckner, R.L., Fischl, B., 2009. Regional white matter volume differences in nondemented aging and Alzheimer's disease. NeuroImage 44, 1247–1258.

Sastre-Janer, F.A., Regis, J., Belin, P., Mangin, J.F., Dormont, D., Masure, M.C., Remy, P., Frouin, V., Samson, Y., 1998. Three-dimensional reconstruction of the human

central sulcus reveals a morphological correlate of the hand area. Cereb. Cortex 8, 641–647.
Sled, J.G., Zijdenbos, A.P., Evans, A.C., 1998. A nonparametric method for automatic correction of intensity nonuniformity in MRI data. IEEE Trans. Med. Imaging 17, 87–97.
Taki, Y., Goto, R., Evans, A., Zijdenbos, A., Neelin, P., Lerch, J., Sato, K., Ono, S., Kinomura, S., Nakagawa, M., Sugiura, M., Watanabe, J., Kawashima, R., Fukuda, H., 2004. Voxel-based morphometry of human brain with age and cerebrovascular risk factors. Neurobiol. Aging 25, 455–463.
Talairach, J. (Ed.), 1988. Co-planar Stereotaxic Atlas of the Human Brain. Thieme Medical Publishers, New York.
Thompson, P.M., Schwartz, C., Lin, R.T., Khan, A.A., Toga, A.W., 1996. Three-dimensional statistical analysis of sulcal variability in the human brain. J. Neurosci. 16, 4261–4274.
Thompson, P.M., Moussai, J., Zohoori, S., Goldkorn, A., Khan, A.A., Mega, M.S., Small, G.W., Cummings, J.L., Toga, A.W., 1998. Cortical variability and asymmetry in normal aging and Alzheimer's disease. Cereb. Cortex 8, 492–509.
White, L.E., Andrews, T.J., Hulette, C., Richards, A., Groelle, M., Paydarfar, J., Purves, D., 1997a. Structure of the human sensorimotor system. I: morphology and cytoarchitecture of the central sulcus. Cereb. Cortex 7, 18–30.
White, L.E., Andrews, T.J., Hulette, C., Richards, A., Groelle, M., Paydarfar, J., Purves, D., 1997b. Structure of the human sensorimotor system. II: lateral symmetry. Cereb. Cortex 7, 31–47.
Wu, Y.C., Field, A.S., Whalen, P.J., Alexander, A.L., 2010. Age- and gender-related changes in the normal human brain using hybrid diffusion imaging (HYDI). NeuroImage 54, 1840–1853.